

Vibrational Quenching of CN^- in Collisions with He and Ar

Barry Mant,¹ Ersin Yurtsever,² Lola González-Sánchez,³ Roland Wester,¹ and Franco A. Gianturco^{1, a)}

¹⁾*Institute for Ion Physics and Applied Physics, University of Innsbruck, Technikerstr. 25/3, 6020 Innsbruck, Austria*

²⁾*Department of Chemistry, Koç University, Rumelifeneri yolu, Sariyer, TR-34450, Istanbul, Turkey*

³⁾*Departamento de Química Física, University of Salamanca, Plaza de los Caídos sn, 37008 Salamanca, Spain*

(Dated: 21 January 2021)

The vibrational quenching cross sections and corresponding low-temperature rate constants for the $v = 1$ and $v = 2$ states of CN^- ($^1\Sigma^+$) colliding with He and Ar atoms have been computed *ab initio* using new three dimensional potential energy surfaces. Little work has so far been carried out on low-energy vibrationally inelastic collisions for anions with neutral atoms. The cross sections and rates calculated at energies and temperatures relevant for both ion traps and astrochemical modelling, are found by the present calculations to be even smaller than those of the similar C_2^-/He and C_2^-/Ar systems which are in turn of the order of those existing for the collisions involving neutral diatom-atom systems. The implications of our finding in the present case rather small computed rate constants are discussed for their possible role in the dynamics of molecular cooling and in the evolution of astrochemical modelling networks.

I. INTRODUCTION

Vibrationally inelastic collisions are fundamental processes in chemical physics and molecular dynamics. Gas phase collisions which can excite or quench a vibrational mode in a molecule have been studied both experimentally and theoretically for decades^{1–5} and are generally well understood. Typically the scattering cross sections and corresponding rates are relatively small⁶ due to the generally large energy spacing between vibrational levels which require strong interaction forces between the colliding species to induce transitions. On the other hand, these processes still attract a great deal of attention and study as they have important applications in fields such as cold molecules, where collisions are used to quench internal molecular motion,^{7–9} or astrochemistry, where accurate rate constants are necessary to model the evolution of gas clouds and atmospheres.^{10–14} There are also exceptional systems such as the dramatic case of $\text{BaCl}^+ + \text{Ca}$ where laser cooled calcium atoms can efficiently quench vibrational motion with rates similar to rotational transitions.^{9,15}

There continues to be many studies of diatom-atom vibrationally inelastic collisions for both neutral^{7,11,16,17} and cationic species.^{15,18–20} This is to be contrasted by with the case for anions, where very little work has been carried out on vibrationally inelastic collision processes. Recently we have tried to change this trend and have investigated vibrational quenching of the C_2^- anion in collisions with noble gas atoms.²¹ This molecule is of direct interest as a possible candidate for laser cooling mechanisms²² but a first step will require the cooling of internal motion via collisions since spontaneous dipole emission is forbidden for the rovibrational excited states of this homonuclear species. The cross sections and rate constants for vibrational transitions were found by our calculations to be small, i.e. of the order of those for neutral species.

In this article we report the vibrational quenching of yet another important anion, CN^- in collisions with He and Ar atoms. The cyanide anion is a well studied molecule, particularly its spectroscopic properties have attracted a great deal of attention and investigations^{23–28} as well as the determination of its photodetachment energy^{23,29,30}. Recent work in our group has further clarified important aspects of its photodetachment behaviour at threshold from cold trap experiments.³¹ This molecule has also been detected in the envelope of a carbon star³² after its rotational constants were carefully measured.²⁵ Collisional processes of the anion with the astrochemically relevant He and H_2 species^{33,34} for rotational transitions have recently been studied and we have also investigated the rotational cooling of this molecular anion with He, Ar and H_2 as buffer gases.³⁵ The CN^- anion is also thought to be an important participant as well in reactions in the interstellar medium^{36–39} and in the atmosphere of Titan⁴⁰ where it has been detected.^{41,42}

We note in passing that the corresponding neutral species CN was one of the first molecules to be detected in space⁴³ and cross sections and rates for this species have been investigated and obtained for various ro-vibrational processes in collisions with He and H_2 .^{16,44–49} The cyanide cation is also suspected to be important to astrochemical processes but has yet to be detected. The cation's vibrational energies have recently been measured⁵⁰ as well as a study has been carried out on its rotational transitions induced by He collisions.⁵¹

Vibrationally inelastic collisions involving the CN^- molecular anion with neutral atoms are a type of process rarely studied for such systems. Although CN^- can of course lose energy through spontaneous emission, its wide relevance justifies providing an accurate assessment of the vibrational quenching processes involving He and Ar, typical buffer gases in ion traps.

The paper is organised as follows: Section II presents the CN^- potential energy and dipole moment curves along with the anion's vibrational energy levels and Einstein A coefficients. The potential energy surfaces for the CN^-/He and CN^-/Ar systems are then discussed in Section III. The quan-

^{a)}Electronic mail: francesco.gianturco@uibk.ac.at

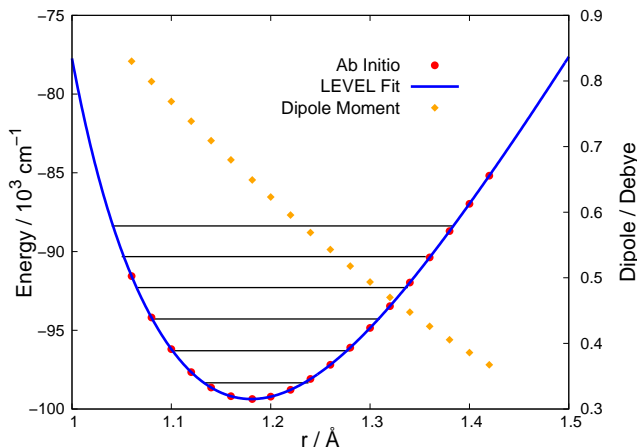


FIG. 1. *Ab initio* energies, PEC fit and DMC for CN^- ($^1\Sigma^+$). The horizontal lines show the first six vibrational energies.

tum scattering methodology is described in Section IV and scattering cross sections and rates are discussed in Section V. Conclusions are given in Section VI.

II. CN^- POTENTIAL ENERGY CURVE AND DIPOLE MOMENT

Electronic energies for the ground $^1\Sigma^+$ state of the CN^- anion were calculated at 19 internuclear distances r to obtain the anion's potential energy curve (PEC). Calculations were carried out using the MOLPRO suite of quantum chemistry codes^{52,53} at the CCSD(T) level of theory^{54,55} employing an aug-cc-pV5Z basis set.^{56,57} The expectation value of the non-relaxed CCSD dipole moment at each r distance was also obtained. The *ab initio* energies and dipole moment curve (DMC) for CN^- are shown in Fig. 1.

The LEVEL program⁵⁸ was used to obtain the vibrational energies and wavefunctions, for the CN^- molecule. The *ab initio* energies were used as input, interpolated using a cubic spline and extrapolated to r values below and above the range of calculated energies using functions implemented in LEVEL. The relative energies of the first three vibrational levels along with the rotational constants for each state are shown in Table I and compared with previously published calculated theoretical and experiment values. The agreement with previous calculations and experimental values is quite good and certainly sufficient to evaluate the cross sections and rate constants of inelastic collisions considered below.

We have recently evaluated the dipole moment of CN^- at its equilibrium bond length r_{eq} using a variety of *ab initio* methods and basis sets³³ and used it to evaluate the Einstein A coefficients for pure rotational transitions. The best estimate of that work of 0.71 D is in quite good agreement with the value of the DMC at r_e of 0.65 D computed here. The LEVEL program was also used to calculate the Einstein A coefficients for ro-vibrational transitions of CN^- using the *ab initio* calculated DMC. The values of $A_{v',j',v'',j''}$ for the first two vibrational states of the anion are shown in Table II and com-

TABLE I. Comparison of vibrational energies and rotational constants with previous theoretical and experimental values. Literature values calculated from Dunham parameters provided. Units of cm^{-1} .

		Relative energy	B_v
v_0	This work	0	1.864
	Calc. ²⁸	0	1.868
	Exp. ²⁵	0	1.872
v_1	This work	2040	1.845
	Calc. ²⁸	2045	1.851
	Exp. ²³	2035 (± 40)	
	Exp. ²⁴	2053 (Neon)	
v_2	This work	4055	1.831
	Calc. ²⁸	4065	1.834

pared to those of neutral CN .⁵⁹ The values for the anion and neutral molecule are broadly similar which is reasonable considering they have very similar bond lengths and vibrational energies.⁵⁹ The slightly larger values for neutral CN are a result of the larger dipole moment for the neutral molecule.⁵⁹

TABLE II. Einstein A coefficients $A_{v',j',v'',j''}$ for selected CN^- ($^1\Sigma^+$) vibrational transitions compared to those for neutral CN ($^2\Sigma^+$) calculated by Brooke *et al.*⁵⁹ For CN^- the P(1) branch values were used to compare to the Q-branch values for CN . Units of s^{-1} .

Transition	CN^-	CN
$v_1 \rightarrow v_0$	6.60	8.85
$v_2 \rightarrow v_1$	12.50	16.50
$v_2 \rightarrow v_0$	0.36	0.66

III. CN^-/He AND CN^-/Ar POTENTIAL ENERGY SURFACES AND VIBRATIONALLY AVERAGED MATRIX ELEMENTS

The interaction energies between CN^- in its ground $^1\Sigma^+$ electronic state with He and Ar atoms were calculated using *ab initio* methods implemented in the MOLPRO suite of codes.^{52,53} Geometries were defined on a Jacobi grid with R (the distance from the centre of mass of CN^- to the atom) ranging from 2.5 to 20 Å and θ (the angle between R and the CN^- internuclear axis r) from 0 (C side) to 180° in 15° and 10° intervals for He and Ar respectively. Seven values of the CN^- bond length for each system between $r = 1.00$ -1.42 Å were used including the equilibrium value of $r_{eq} = 1.181431$ Å. This is sufficient to cover the vibrational levels of interest in the present study. Interaction potential energies between CN^- and the noble gas atoms were determined by subtracting the asymptotic energies for each bond length.

For CN^-/He , energies were calculated using the Multi-configurational self-consistent field (MCSCF) method^{60,61} with 8 occupied orbitals and 2 closed orbitals followed by a 1-state multi-reference configuration interaction (MRCI)⁶² calculation. An aug-cc-pV5Z basis⁶³ was employed. In our

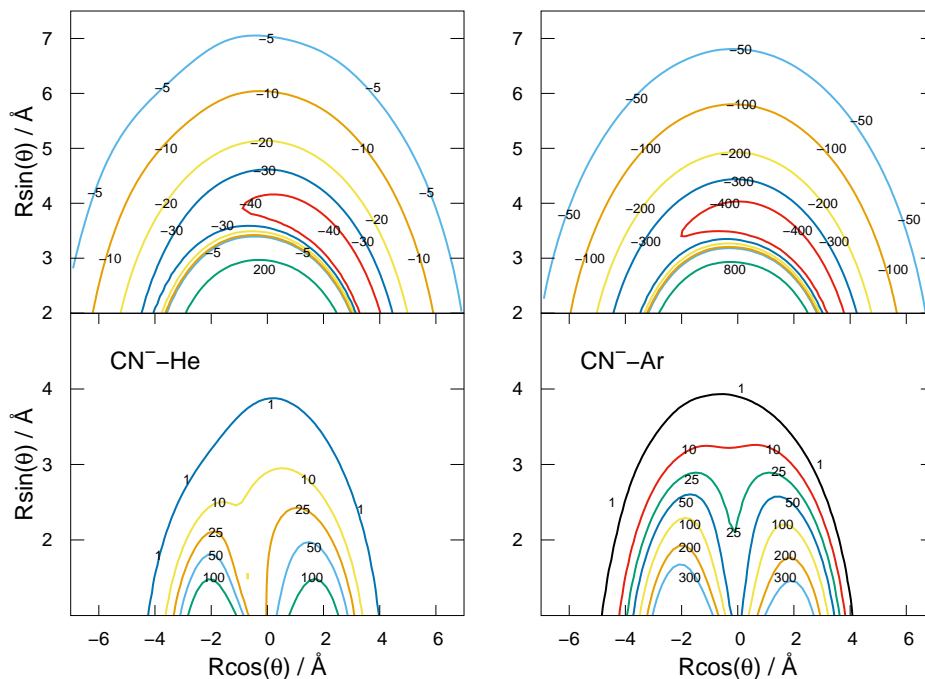


FIG. 2. Contour plots for $\text{CN}^-({}^1\Sigma^+)/\text{He}$ (left) and $\text{CN}^-({}^1\Sigma^+)/\text{Ar}$ (right) of vibrationally averaged matrix elements $V_{0,0}(R, \theta)$ (top) and $V_{0,1}(R, \theta)$ (bottom) projected onto Cartesian coordinates. Energies in cm^{-1} . See main text for further details

earlier discussion of the CN^-/He PES³³ we discuss in detail the reasons why we followed both methods for this system and compared the CASSCF+MRCI results with the CCSD(T) with similar basis set expansions, finding them to be coincident in values. In particular, we corrected for the size-consistency possible shortcomings of the CASSCF+MRCI vs the CCSD(T) methods by correcting the latter results using the Davidson's correction as implemented in MOLPRO. In our earlier work³³ we showed that this correction brought the two sets of potential calculations to yield the same potential values over a broad range of the employed grid. As an example, we note here that from our CBS (Complete Basis Set) extrapolated CCSD(T) calculations on CN^-/He system we find the minimum energy configuration as $\theta=40$ deg., $R=3.95$ Å with BSSE corrected energy at 49.522 cm^{-1} . CBS is calculated by the default procedure in MOLPRO: it is the so-called L3 extrapolation discussed in there. The results within the CAS(8,4) within the CASSCF+MRCI gave a $\theta=40$ deg., $R=4.00$ and an energy of 50.39 cm^{-1} for its minimum configuration, showing the two methods to provide essentially the same results.

For the CN^-/Ar system, energies were calculated using the CCSD(T) method⁵⁵ with complete basis set (CBS) extrapolation using the aug-cc-pVTZ, aug-cc-pVQZ and aug-cc-pV5Z basis sets.^{56,64} The basis-set-superposition-error (BSSE) was also accounted for all calculated points using the counterpoise procedure.⁶⁵

The three-dimensional PESs were fit to an analytical form using the method of Werner, Follme and Alexander^{11,66}

where the interaction energy is given as

$$V_{\text{int}}(R, r, \theta) = \sum_{n=0}^{N_r-1} \sum_{l=0}^{N_\theta-1} P_l(\cos \theta) A_{ln}(R) (r - r_{eq})^n, \quad (1)$$

where $N_r = 7$ and $N_\theta = 13$ or 19 respectively are the number of bond lengths r and angles θ in the *ab initio* grid, $P_l(\cos \theta)$ are the Legendre polynomials and $r_{eq} = 1.181431$ Å is the equilibrium bond length of CN^- . For each bond length r_m and angle θ_k , one-dimensional cuts of the PESs $V_{\text{int}}(R, r_m, \theta_k)$ were fit to

$$B_{km}(R) = \exp(-a_{km}R) \left[\sum_{i=0}^{i_{\text{max}}} b_{km}^{(i)} R^i \right] - \frac{1}{2} [1 + \tanh(R)] \left[\sum_{j=j_{\text{min}}}^{j_{\text{max}}} c_{km}^j R^{-j} \right], \quad (2)$$

where the first terms account for the short range part of the potential and the second part for the long range terms combined using the $\frac{1}{2} [1 + \tanh(R)]$ switching function. For each r_m and θ_k Eq. 2 was least squares fit to the *ab initio* data (around 40 R points) using $i_{\text{max}} = 2$, $j_{\text{min}} = 4$ and $j_{\text{max}} = 10$ for eight variable parameters. The average root-mean-square error (RMSE) for each fit was 0.21 cm^{-1} for CN^-/He and 0.27 cm^{-1} for CN^-/Ar . From the 1D potential fits $B_{km}(R)$, the radial coefficients $A_{ln}(R)$ can be determined from the matrix product $\mathbf{A}(R) = \mathbf{P}^{-1} \mathbf{B}(R) \mathbf{S}^{-1}$ where the matrix elements of \mathbf{P} and \mathbf{S} are given as $P_{kl} = P_l(\cos \theta_k)$ and $S_{nm} = (r_m - r_{eq})^n$ respectively. The analytical representation of the PES, Eq. 1, gives a reasonable representation of the *ab initio* interaction energies. An overall RMSE of 82 cm^{-1} for all points used in the fit was obtained for CN^-/He but this drops to 0.26

cm^{-1} for $V < 500 \text{ cm}^{-1}$. For CN^-/Ar an overall RMSE of 21 cm^{-1} was obtained, a value which went down to 1.5 cm^{-1} for $V < 500 \text{ cm}^{-1}$.

The scattering calculations described in the next section require the interaction potential to be averaged over the vibrational states of CN^- $\chi_v(r)$, which were obtained from LEVEL as described in Section II, as

$$V_{v,v'}(R, \theta) = \langle \chi_v(r) | V_{\text{int}}(R, r, \theta) | \chi_{v'}(r) \rangle. \quad (3)$$

Fig. 2 shows the diagonal terms $V_{0,0}(R, \theta)$ for both systems. As expected for a molecule with a strong bond, so that the ground state vibrational wavefunction is strongly peaked around r_{eq} , the contour plots of the $V_{0,0}(R, \theta)$ for each system are very similar to our earlier rigid-rotor (RR) PESs which were obtained without the vibrational averaging.^{33,35} Both system's PES have a fairly similar appearance with the most attractive part of the potential located on the nitrogen end of CN^- . The well depth is the main difference which increases as expected from He to Ar due to the increasing number of electrons on the atoms and on the much larger dipole polarizability that dominates the long-range attractive terms with a value of $1.383 a_0^3$ for He and $11.070 a_0^3$ for Ar.⁶⁷

The off diagonal $V_{0,1}(R, \theta)$ terms which directly drive vibrationally inelastic $v = 1$ to $v = 0$ transitions are also shown in Fig. 2. At short distances the coupling terms are repulsive, becoming negligible rather quickly at longer distances, as is the case for many other atom-diatom systems where the vibrational coupling features are largely short-range coupling regions. The interaction of CN^- with Ar is more repulsive at close range and for a broader range of geometries than is the case for He. These findings suggest already that low-energy collisions with Ar will be likely to induce larger vibrational cross sections than for the same collisions involving He atoms. Such expected behaviour will be in fact confirmed below by our actual calculations.

The PESs for CN^-/He and CN^-/Ar can be compared to similar systems such as C_2^-/He and C_2^-/Ar which we have recently investigated.²¹ The location of the minimum interaction energy for both anions interacting with He and Ar respectively are very similar with the main difference being the perpendicular angle of the well for C_2^- . The off-diagonal matrix elements for these systems are also similar in magnitude and range but being slightly larger for the interaction of He and Ar with C_2^- , explaining the larger quenching rates for this anion (see below). The PES for the corresponding neutral systems CN/He and CN/Ar which were reported by Saidani *et al.* can also be compared.⁶⁸ In this case the well depth for He interacting with both CN and CN^- is similar but for Ar the interaction with the anion is somewhat weaker. As expected the interaction potential for He and Ar interacting with the anion extends further than the corresponding neutral systems. The off-diagonal elements for the neutral and anionic systems are broadly similar.

The close-coupling (CC) scattering calculations to be discussed in the next section require to have the vibrationally averaged matrix elements in the form of the familiar multipole

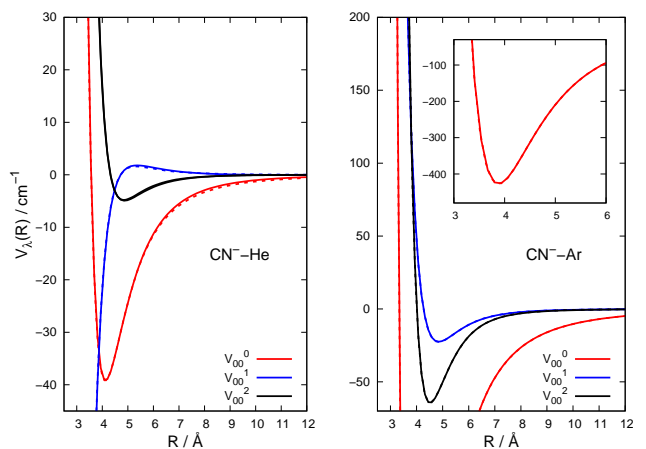


FIG. 3. $V_{0,0}^\lambda(R)$ expansion coefficients for $\lambda = 0, 1$ and 2 terms for CN^-/He (left) and CN^-/Ar (right). The rigid rotor (RR) values are also plotted as dashed lines but essentially overlap the vibrationally averaged coefficients discussed in the present work.

expansion given as

$$V_{v,v'}(R, \theta) = \sum_{\lambda}^{\lambda_{\text{max}}} V_{v,v'}^\lambda(R) P_\lambda(\cos \theta). \quad (4)$$

Fig. 3 shows the multipole expansion coefficients for the first three $V_{0,0}(R, \theta)$ terms for both systems. As anticipated from the broad spatial similarity of the contour plots, the multipole expansion for the vibrationally averaged matrix elements are very close to those obtained from considering the anion as a rigid rotor. This justifies our previous treatment of purely rotationally inelastic transitions where we considered the anion to behave as a rigid rotor (RR)^{33,35} and we refer the reader to these works for a discussion of pure rotational transitions.

It is also worthy of note about the diagonal coupling matrix elements reported in that Fig. 3 how the much more polarizable Ar projectile gives the three lowest multipolar terms as attractive contributions to the interaction, thereby indicating that their collective effects during the interaction would be to draw the heavier partner closer to the anion. On the other hand, the same three coefficients for the lighter He partner (left-hand panel in Fig. 3) exhibit much shallower attractive wells and only for two of the coefficients, with the $\lambda = 1$ coefficient showing instead a slightly repulsive behaviour at intermediate distances.

The off-diagonal expansion coefficients $V_{0,1}^\lambda$ are shown in Fig. 4. All terms quickly approach zero as R is increased. For both systems the $V_{0,1}^\lambda(R)$ coefficients are mostly steeply repulsive as R decreases. As expected from the contour plots, the $V_{0,1}^\lambda(R)$ terms are seen to be much more repulsive for the CN^-/Ar interaction, with their turning points located at larger distances than happens for the He partner. Such features of the interactions again suggest a larger dynamical vibrational inelasticity for the case of Ar atoms than for the He collision partners.

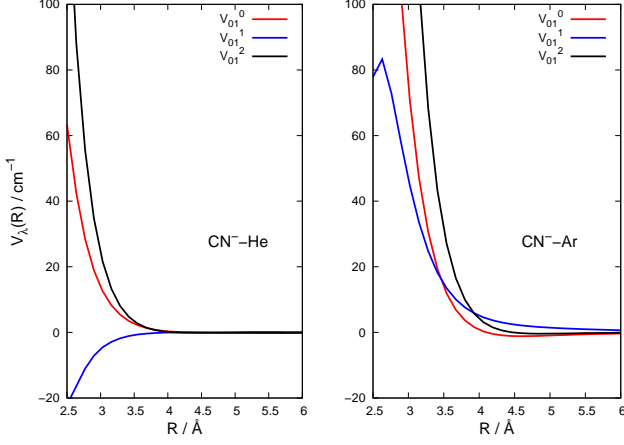


FIG. 4. $V_{1,0}^{\lambda}(R)$ expansion coefficients for $\lambda = 0, 1$ and 2 terms for CN^{-}/He (left) and CN^{-}/Ar (right).

IV. QUANTUM SCATTERING CALCULATIONS

Quantum scattering calculations were carried out using the coupled channel (CC) method to solve the Schrödinger equation for scattering of an atom with a diatomic molecule as implemented in our in-house code, ASPIN.⁶⁹ The method has been described in detail many times before, from one of its earliest, now classic formulations⁷⁰ to one of its more recent, computation-oriented visitation from our own work⁶⁹. Therefore, only a brief summary of the method will be given here with all equations given in atomic units. By starting with the form employed for any given total angular momentum $\mathbf{J} = \mathbf{l} + \mathbf{j}$ the scattering wavefunction is expanded as

$$\Psi^{JM}(R, r, \Theta) = \frac{1}{R} \sum_{v,j,l} f_{vlj}^J(R) \chi_{v,j}(r) \mathcal{Y}_{jl}^{JM}(\hat{\mathbf{R}}, \hat{\mathbf{r}}), \quad (5)$$

where l and j are the orbital and rotational angular momentum respectively, $\mathcal{Y}_{jl}^{JM}(\hat{\mathbf{R}}, \hat{\mathbf{r}})$ are coupled-spherical harmonics for l and j which are eigenfunctions of J . $\chi_{v,j}(r)$ are the radial part of the ro-vibrational eigenfunctions of the molecule. The values of l and j are constrained, via Clebsch-Gordan coefficients, such that their final summation is compatible with the specific total angular momentum J one is considering.^{69,70} $f_{vlj}^J(R)$ are the radial expansion functions which need to be determined from the propagation of the radial coupled equations.

Substituting the expansion into the Schrödinger equation with the Hamiltonian for atom-diatom scattering as defined in detail in^{69,70}, leads to the CC equations for each contributing J

$$\left(\frac{d^2}{dR^2} + \mathbf{K}^2 - \mathbf{V} - \frac{\mathbf{I}^2}{R^2} \right) \mathbf{f}^J = 0. \quad (6)$$

Here each element of $\mathbf{K} = \delta_{i,j} 2\mu(E - \varepsilon_i)$ (where ε_i is the channel asymptotic energy), μ is the reduced mass of the system, $\mathbf{V} = 2\mu\mathbf{U}$ is the interaction potential matrix between channels and \mathbf{I}^2 is the matrix of orbital angular momentum.

For the ro-vibrational scattering calculations of interest in the present study, the matrix elements \mathbf{U} are given explicitly as

$$\langle v j l J | V | v' j' l' J \rangle = \int_0^\infty dr \int d\hat{\mathbf{r}} \int d\hat{\mathbf{R}} \chi_{v,j}(r) \mathcal{Y}_{jl}^{JM}(\hat{\mathbf{R}}, \hat{\mathbf{r}})^* |V(R, r, \theta)| \chi_{v',j'}(r) \mathcal{Y}_{j'l'}^{JM}(\hat{\mathbf{R}}, \hat{\mathbf{r}}). \quad (7)$$

Since the intermolecular potential $V(R, r, \theta)$ is expressed as in Eq. 4, then Eq. 7 can be written as

$$\langle v j l J | V | v' j' l' J \rangle = \sum_{\lambda=0}^{\infty} V_{v,v'}^{\lambda}(R) f_{\lambda,jl,j'l'}^J, \quad (8)$$

where the $f_{\lambda,jl,j'l'}^J$ terms are the Percival-Seaton coefficients

$$f_{\lambda,jl,j'l'}^J = \int d\hat{\mathbf{r}} \int d\hat{\mathbf{R}} \mathcal{Y}_{jl}^{JM}(\hat{\mathbf{R}}, \hat{\mathbf{r}})^* P_{\lambda}(\cos \theta) \mathcal{Y}_{j'l'}^{JM}(\hat{\mathbf{R}}, \hat{\mathbf{r}}), \quad (9)$$

for which analytical forms are known.⁶⁹ Eq. 8 also makes use of the widely known approximation

$$V_{v,v'}^{\lambda}(R) \approx V_{v,jv',j'}^{\lambda}(R), \quad (10)$$

for all j such that the effect of rotation on the vibrational matrix elements is ignored for reasons that shall be further discussed below.

The CC equations are propagated outwards from the classically forbidden region to a sufficient distance where the scattering matrix \mathbf{S} can be obtained. The inelastic ro-vibrational state-changing cross sections are obtained as

$$\sigma_{v_j \rightarrow v' j'} = \frac{\pi}{(2j+1)k_{vj}^2} \sum_J (2J+1) \sum_{l,l'} |\delta_{vlj, v'l'j'} - S_{vlj, v'l'j'}^J|^2. \quad (11)$$

To converge the CC equations, a rotational basis set was also used: for both systems it included up to $j = 20$ rotational functions for each vibrational state. The CC equations were propagated between 1.7 and 100.0 Å using the log-derivative propagator⁷¹ up to 60 Å and the variable-phase method at larger distances.⁷² The potential energy was interpolated between calculated $V_{v,v'}^{\lambda}(R)$ values using a cubic spline. For $R < 2.5$ Å the $V_{v,v'}^{\lambda}(R)$ were extrapolated as $\frac{a_{\lambda}}{R} + b_{\lambda}R$ while for $R > 20$ Å the $\lambda = 0$ terms were extrapolated as $\frac{c}{R^4} + \frac{d}{R^6}$. As our *ab initio* calculated interaction energies were computed to $R = 25$ Å where the interaction energy is negligible for the temperatures of interest here, the extrapolated form has also a negligible effect on cross sections.⁷³

A number of parameters of the calculation were checked for convergence. The scattering cross sections differed by around 10-15% on going from 10 to 19 λ terms. This is less precise than for rotationally inelastic cross sections where convergence to around 1% is typical and is due to the very small cross sections for these processes which makes obtaining precise and stable values more difficult to achieve. For production calculations, 10 λ terms were included for each $V_{v,v'}(R)$ as a compromise between accuracy and computational time. The effect of the vibrational basis set was also considered. It was found that for the $v = 1$ and $v = 2$ levels, which are the states of interest here (see next section), it was sufficient

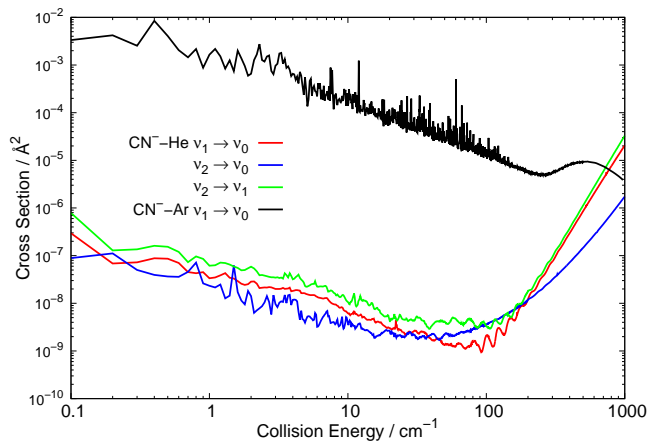


FIG. 5. Scattering cross sections for vibrationally inelastic collisions of CN^- with He and Ar.

to only include these states. Including the $v = 3$ state had a negligible effect on the $v = 1$ and $v = 2$ quenching cross sections. The rotational $j = 20$ basis gave convergence to better than 1% for the CN^-/He while for CN^-/Ar convergence to about 10% was achieved.

Scattering calculations were carried out for collision energies between 1 and 1000 cm^{-1} using steps of 0.1 cm^{-1} for energies up to 100 cm^{-1} , 0.2 cm^{-1} for $100\text{-}300 \text{ cm}^{-1}$, 1.0 cm^{-1} for $300\text{-}500 \text{ cm}^{-1}$ and 10.0 cm^{-1} for $500\text{-}1000 \text{ cm}^{-1}$. This energy grid was used to ensure that important features such as resonances appearing in the cross sections were accounted for and their contributions included when the corresponding rates were calculated. At low collision energies, the positions and widths of such resonances will be very sensitive to the details of the PES.

For CN^-/Ar the number of partial waves was increased with increasing energy as usual, requiring $J = 120$ for the highest energies considered. For the CN^-/He system however, inverse behaviour was encountered: at low scattering energies below 100 cm^{-1} , more partial waves were required (up to $J = 80$) to converge the vibrationally inelastic partial cross sections than at higher energies where only up to $J = 35$ was required. We suspect this is due to the very small cross sections so that at low energies it becomes difficult to converge the calculations as all partial waves contribute uniformly very small values so that many more of them need inclusion for an acceptable convergent behaviour to occur.

Vibrationally inelastic cross sections were computed for the $v = 1$ and $v = 2$ states of CN^- for collisions with He. Due to time and memory constraints, only $v = 1$ states of CN^- were considered for Ar collisions. We think, however, that such calculations are already sufficient for our results to make convincingly our main points, as discussed further below.

V. VIBRATIONALLY INELASTIC CROSS SECTIONS & RATE COEFFICIENTS

Fig. 5 compares vibrationally inelastic rotationally elastic (for $j = j' = 0$) cross sections for the de-excitation $v = 1 \rightarrow v = 0$, $v = 2 \rightarrow v = 1$ and $v = 2 \rightarrow v = 0$ transitions for CN^- colliding with He and $v = 1 \rightarrow v = 0$ for CN^-/Ar . At low collision energies below 100 cm^{-1} the cross sections for He are very small, orders of magnitude less than rotationally inelastic collisions for this system.³³ The cross sections show resonances at lower collision energies due to shape and/or Feshbach resonances. As expected due to the larger energy difference, the $v = 2 \rightarrow v = 0$ process is smaller than the $v = 2 \rightarrow v = 1$ and $v = 1 \rightarrow v = 0$ cross sections. At collision energies above 100 cm^{-1} , the cross sections rapidly increase in value, a behaviour typically observed also in other systems for vibrationally inelastic cross sections.¹¹⁻¹⁴

The CN^-/Ar cross sections are found to be about four orders of magnitude larger than those we have obtained for He at lower energies, also showing many distinct resonance features which are brought about by the presence of a stronger interaction with the molecular anion. The detailed analysis of such a forest of resonances would also be interesting and perhaps would be warranted in the case of existing experimental data on such processes, of which we are not aware till now, but would require a substantial extension of the present work. Thus, we do not intend to carry it out now, being somewhat outside the main scope of the present study, and are leaving it for future extension of this study in our own laboratory.

The far larger cross sections we found for the Ar projectile are obviously a consequence of the deeper attractive well for the $V_{v,v}(R, \theta)$ diagonal matrix elements and the larger off-diagonal $V_{v,v'}(R, \theta)$ matrix elements (see Fig. 2), i.e. they stem from distinct differences in the strengths of the coupling potential terms that drive the inelastic dynamics for the Ar collision partner.

The general features of the vibrationally inelastic cross sections shown in Fig. 5 are indeed similar to those which we have obtained earlier for the C_2^- anion colliding with He, Ne and Ar set of systems that we have recently studied.²¹ For both of the anions, we have found that the vibrational quenching cross sections with He are uniformly very small, while we also found that they increase by orders of magnitude when the larger and more polarizable Ar atom becomes the collisional partner for either of these anionic molecules. Although such general behaviour could be reasonably expected from what we know in these systems about their interaction forces, it is nevertheless reassuring to obtain quantitative confirmation on the extent of the size differences from detailed, and in principle exact, scattering calculations.

The computed inelastic cross sections of the previous section can in turn be used to obtain the corresponding thermal rate constants over ranges of temperature of interest for placing the present anion in cold environments. The corresponding $k_{v \rightarrow v'}(T)$ can be evaluated, in fact, as the convolution of the computed inelastic cross sections over a Boltzmann distribution of the relative collision energies of the interacting partners as

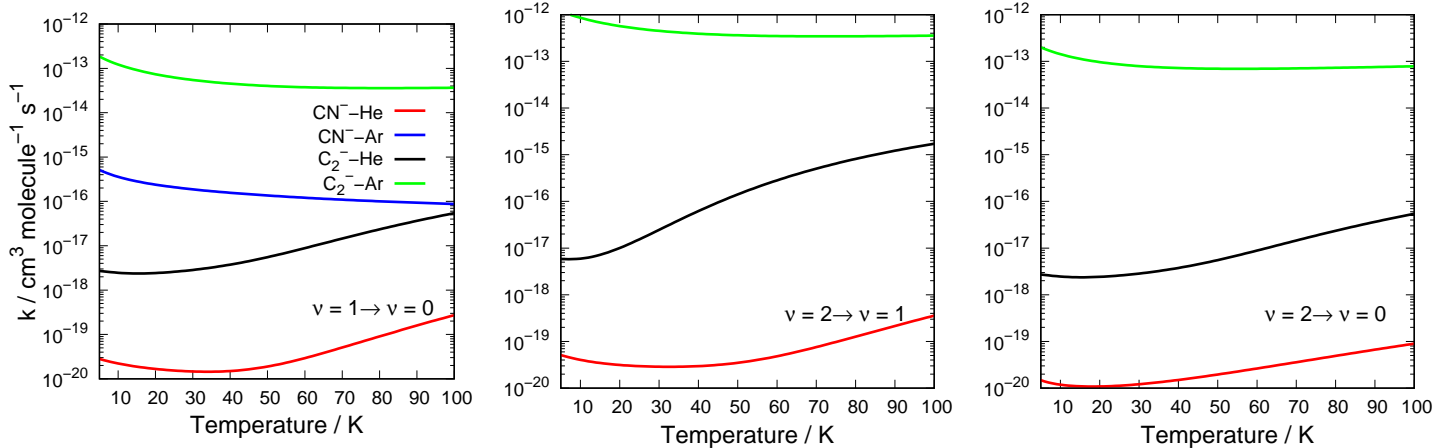


FIG. 6. Rate constants $k_{v \rightarrow v'}(T)$ for vibrationally inelastic transitions in CN^-/He and Ar collisions. Also shown are the corresponding values for C_2^-/He and Ar.²¹

$$k_{v \rightarrow v'}(T) = \left(\frac{8}{\pi \mu k_B^3 T^3} \right)^{1/2} \int_0^\infty E_c \sigma_{v \rightarrow v'}(E_c) e^{-E_c/k_B T} dE_c \quad (12)$$

where $E_c = \mu v^2/2$ is the kinetic energy in the collision calculations. The rate constants were computed between 5 and 100 K in 1 K intervals. Fig. 6 shows the rates for vibrationally inelastic rotationally elastic ($j = j' = 0$) transitions corresponding to the cross sections in Fig. 5. The figure also shows rates for the corresponding transitions of the similar C_2^-/He and Ar systems. For CN^-/He the rate constants for vibrational quenching are very small, even lower than those for C_2^-/He and around nine orders of magnitude lower than those for CN^-/He rotationally inelastic collisions.³³ For CN^-/Ar the $v = 1 \rightarrow v = 0$ rate constants are about four orders of magnitude larger than those for He but about three orders of magnitude less than for the corresponding transition for C_2^-/Ar . The $v = 2 \rightarrow v = 1$ rate constants for CN^-/He is broadly similar to those for $v = 1 \rightarrow v = 0$ while as expected the $v = 2 \rightarrow v = 0$ rate constants are slightly smaller.

The increase in rate constants on going from He to Ar in collisions are similar to what was found for rotationally inelastic collisions for CN^- ³⁵ and C_2^- ⁷⁴ and as shown in Fig. 6, vibrationally inelastic collisions for C_2^- .²¹ This trend, while seemingly in expectation with the stronger interaction potential for the larger atom is not easy to predict *a priori*. Kato *et al.* and Ferguson measured vibrational quenching rates for N_2^+ in collisions with He, Ne, Ar, Xe and Kr⁷⁵ and O_2^+ with He, Ne and Ar atoms⁷⁶ respectively at 300 K. For both cations, quenching rates increased with the size of atom, suggesting that the polarizability of the colliding atom plays an important role. In contrast Saidani *et al* calculated quenching rates for CN with He and Ar over a wide range of temperatures

and found that cross sections and rates for Ar were orders of magnitude lower than those for He.⁶⁸ However, ionic interactions are driven by different forces than those acting between neutrals, so it is not obvious how such a result relates to the present findings for an anion. Analytical models can also be used to gain insight into vibrational quenching such as the work of Dashevskaya *et al.* where the quenching rate for $v = 1 \rightarrow v = 0$ for N_2/He was calculated over a large range of temperatures from 70-3000 K.⁷⁷ The rates obtained were in good agreement with experiment and similar to those found here for CN^-/He at 100 K. It would be interesting to apply these models to the anion-neutral collisions of interest here.

The work we have presented here, and the similar findings from our previous study²¹ on a different diatomic anion like C_2^- , strongly suggests that the process of vibrational inelasticity in multiply bonded anionic molecules by low-T collisions with neutral noble gases is rather inefficient. The rates for quenching found here are even smaller than those we had found earlier for C_2^- , also uniformly smaller than those known for many neutral diatomic molecules and cations²¹.

The quenching rates and Einstein A coefficients which we have mentioned and shown earlier in this work, can be used to consider the properties of the critical density $n_{\text{crit}}^i(T)$ for CN^- vibrations which is given as

$$n_{\text{crit}}^i(T) = \frac{A_{ij}}{\sum_{j \neq i} k_{ij}(T)}. \quad (13)$$

This quantity gives the gas density values which would be required so that collisional state-changing processes match in size those which lead to collision-less emission via spontaneous decay. It is used in astronomical contexts to assess the possible densities required for local thermal equilibrium (LTE) to be reached and are usually applied for rotational transitions in molecules that can occur in the interstellar medium

(ISM).

In the present case of CN^-/He , when we apply Eq. 13 to the $v = 1$ and $v = 2$ vibrational state-changing process gives $n_{\text{crit}}^i(T) \approx 10^{19} - 10^{20} \text{ cm}^{-3}$ at 100 K. Current kinetics models which describe the density conditions in molecular clouds indicate a wide variety of densities being present: from diffuse molecular clouds estimated at around 10^2 cm^{-3} to dense molecular clouds which are considered to be between $10^3 - 10^6 \text{ cm}^{-3}$.^{78,79} The critical density obtained here for the vibrational decay of CN^- interacting with environmental He atoms was found to be orders of magnitude larger than those expected in the ISM regions where CN^- has been detected, clearly suggesting that thermal equilibrium for these process will likely never be attained and that the presently computed radiative transitions determine that CN^- populates essentially only the ground vibrational level in the ISM.

VI. CONCLUSIONS

The cross sections and corresponding rate constants for vibrationally inelastic transitions of CN^- colliding with He and Ar atoms have been calculated using new *ab initio* potential energy surfaces. As for atom-diatom vibrationally inelastic collisions, the rate constants for both CN^-/He and CN^-/Ar are very small, even smaller than those for corresponding values of the similar C_2^-/He and C_2^-/Ar systems. Although more work is required before definitive conclusions can be drawn, it appears from the present calculations that vibrationally inelastic collisions of molecular anions with neutral atoms (or at least noble gas atoms) are similar to neutral molecule-atom collisions in that they generate similarly small transition probabilities and their collision mechanisms for transferring relative energy, at sub-thermal and thermal conditions, to the vibrational internal motion of the anion is rather inefficient. This is in contrast with the generally more efficient collisional energy transfer probabilities which are found for molecular cation-atom systems in the current literature²¹.

For the anion of interest here this is not a crucial concern when wanting to find alternative paths which are more efficient in cooling its internal vibrational motion, since CN^- can dissipate energy through spontaneous dipole emission (Section II). On the other hand, in the case of homonuclear anions such as C_2^- (of current interest for laser cooling cycles in cold traps²²) where this process is forbidden, collisions are likely to be the primary means for quenching its vibrational motion. In such cases high gas pressures and the use of larger noble buffer gases seem to be required.

The present calculations confirm that collisional energy transfer paths which involve vibrational degrees of freedom for a molecular anion under cold trap conditions are invariably very inefficient and are several orders of magnitude smaller than the collisional energy-changing paths which involve their rotational degrees of freedom. One can therefore safely estimate that these two paths to energy losses are markedly decoupled with one another and can be treated on a separate footing within any kinetics modelling of their behaviour.

ACKNOWLEDGMENTS

We acknowledge the financial support of the Austrian FWF agency through research grant n. P29558-N36. One of us (L.G-S) further thanks MINECO (Spain) for grant PGC2018-09644-B-100.

VII. DATA AVAILABILITY STATEMENT

Fortran programs and subroutines for the CN^-/He and CN^-/Ar PESs used are available in the Supplementary Material along with the vibrational coupling coefficients and vibrational quenching rate constants.

VIII. SUPPLEMENTARY MATERIAL

The multipolar coefficients for the Legendre expansion of the new vibrational PESs for CN^-/He and CN^-/Ar are provided via Fortran program routines, as well as the coupling coefficients for the vibrational dynamics. They are all available as Supplementary Material to the present publication. That Supplementary Material also contains subroutines for the inelastic and elastic rate coefficients for the two systems studied in the present paper.

- ¹K. Takayanagi, "Vibrational and rotational transitions in molecular collisions," *Prog. Theor. Phys. Supp.* **25**, 1–98 (1963).
- ²D. Secrest, "Theory of rotational and vibrational energy transfer in molecules," *Annu. Rev. Phys. Chem.* **24**, 379–406 (1973).
- ³D. J. Krajnovich, C. S. Parmenter, and D. L. Catlett, "State-to-state vibrational transfer in atom-molecule collisions. beams vs. bulbs," *Chem. Rev.* **87**, 237–288 (1987).
- ⁴D. Secrest and B. Robert Johnson, "Exact quantum mechanical calculation of a collision of a particle with a harmonic oscillator," *J. Chem. Phys.* **45**, 4556 (1966).
- ⁵W. Eastes and D. Secrest, "Calculation of rotational and vibrational transitions for the collision of an atom with a rotating vibrating diatomic oscillator," *J. Chem. Phys.* **56**, 640 (1972).
- ⁶W. C. Campbell, G. C. Groenenboom, H.-I. Lu, E. Tsikata, and J. M. Doyle, "Time-domain measurements of spontaneous vibrational decay of magnetically trapped NH," *Phys. Rev. Lett.* **100**, 083003 (2008).
- ⁷I. Kozyryev, L. Baum, K. Matsuda, P. Olson, B. Hemmerling, and J. M. Doyle, "Collisional relaxation of vibrational states of SrOH with He at 2 K," *New J. Phys.* **17**, 045003 (2015).
- ⁸D. Caruso, M. Tacconi, F. A. Gianturco, and E. Yurtsever, "Quenching vibrations by collisions in cold traps: A quantum study for $\text{MgH}^+(X^1\Sigma^+)$ with $^4\text{He}(^1S)$," *J. Chem. Sci.* **124**, 93 (2012).
- ⁹W. Rellergent, S. S. Schowalter, S. Kotochigova, K. Chen, and E. R. Hudson, "Evidence for sympathetic vibrational cooling of translationally cold molecules," *Nature* **495**, 490 (2013).
- ¹⁰F. F. S. van der Tak, F. Lique, A. Faure, J. H. Black, and E. W. van Dishoeck, "The Leiden atomic and molecular database (LAMDA): Current status, recent updates, and future plans," *Atoms* **8**, 2 (2020).
- ¹¹C. Balança and F. Dayou, "Ro-vibrational excitation of SiO by collision with helium at high temperature," *MNRAS* **469**, 1673 (2017).
- ¹²R. Tobiola, F. Lique, J. Klos, and G. Chałasiński, "Ro-vibrational excitation of SiS by He," *J. Phys. B: At. Mol. Opt. Phys.* **41**, 155702 (2008).
- ¹³F. Lique and A. Spielfiedel, "Ro-vibrational excitation of CS by He," *Astron. Astrophys.* **462**, 1179 (2007).
- ¹⁴F. Lique, A. Spielfiedel, G. Dhont, and N. Feautrier, "Ro-vibrational excitation of the SO molecule by collision with the He atom," *Astron. Astrophys.* **458**, 331 (2006).

- ¹⁵T. Stoecklin, P. Halvick, M. A. Gannounim, M. Hochlaf, S. Kotochigova, and E. R. Hudson, "Explanation of efficient quenching of molecular ion vibrational motion by ultracold atoms," *Nat. Commun.* **7**, 11234 (2016).
- ¹⁶B. Yang, X. Wang, P. Stancil, J. Bowman, N. Balakrishnan, and R. Forrey, "Full-dimensional quantum dynamics of rovibrationally inelastic scattering between CN and H₂," *J.Chem.Phys.* **145**, 224307 (2016).
- ¹⁷Y. Kalugina, F. Lique, and S. Marinakis, "New ab initio potential energy surfaces for the ro-vibrational excitation of OH($X^2\Pi$) by He," *Phys. Chem. Chem. Phys.* **16**, 13500 (2014).
- ¹⁸I. Iskandarov, F. A. Gianturco, M. Hernández Vera, R. Wester, H. da Silva Jr., and O. Dulieu, "Shape and strength of dynamical couplings between vibrational levels of the H₂⁺, HD⁺ and D₂⁺ molecular ions in collision with He as a buffer gas," *Eur. Phys. J. D* **71**, 141 (2017).
- ¹⁹T. Stoecklin and A. Voronin, "Vibrational and rotational cooling of NO⁺ in collisions with He," *J. Chem. Phys.* **134**, 204312 (2011).
- ²⁰T. Stoecklin and A. Voronin, "Vibrational and rotational energy transfer of CH⁺ in collisions with ⁴He and ³He," *Eur. Phys. J. D* **46**, 259 (2008).
- ²¹B. P. Mant, F. A. Gianturco, R. Wester, E. Yurtsever, and L. González-Sánchez, "Ro-vibrational quenching of C₂⁻ anions in collisions with He, Ne and Ar atoms," *Phys. Rev. A* **102**, 062810 (2020).
- ²²P. Yzombard, M. Hamamda, S. Gerber, M. Doser, and D. Comparat, "Laser cooling of molecular anions," *Phys. Rev. Lett.* **114**, 213001 (2015).
- ²³S. E. Bradforth, E. H. Kim, D. W. Arnold, and D. M. Nue-mark, "Photoelectron spectroscopy of CN⁻, NCO⁻, and NCS⁻," *J. Chem. Phys.* **98**, 800 (1993).
- ²⁴D. Forney, W. E. Thomson, and E. Jacox, "The vibrational spectra of molecular ions isolated in solid neon. ix. HCN⁺, HNC⁺, and CN⁻" *J. Chem. Phys.* **97**, 1664 (1992).
- ²⁵C. A. Gottlieb, S. Brunken, M. C. McCarthy, and P. Thaddeus, "The rotational spectrum of CN⁻," *J. Chem. Phys.* **126**, 191101 (2007).
- ²⁶P. Botschwina, "Spectroscopic properties of the cyanide ion calculated by SCEP CEPA," *Chem. Phys. Lett.* **114**, 58–62 (1985).
- ²⁷K. A. Peterson and R. Claude Woods, "An *ab initio* investigation of the spectroscopic properties of BCl, CS, CCl⁺, BF, CO, CF⁺, N₂, CN⁻, and NO⁺," *J. Chem. Phys.* **87**, 4409 (1987).
- ²⁸L. T. J and C. E. Dateo, "Accurate spectroscopic characterization of ¹²C¹⁴N⁻, ¹³C¹⁴N⁻, ¹²C¹⁵N⁻," *Spectrochimica Acta Part A* **55**, 739 (1999).
- ²⁹J. Berkowitz, W. A. Chupka, and T. A. Walter, "Photo ionization of HCN: The electron affinity and heat of formation of CN⁻," *J. Chem. Phys.* **50**, 1497 (1969).
- ³⁰R. Klein, R. P. McGinnis, and S. R. Leone, "Photodetachment threshold of CN⁻ by laser optogalvank spectroscopy," *Chem. Phys. Lett.* **100**, 475 (1983).
- ³¹M. Simpson, M. Nötold, A. Schmidt-May, T. Michaelsen, B. Bastian, J. Meyer, R. Wild, F. Gianturco, M. Milovanović, V. Kokoouline, and R. Wester, "Threshold photodetachment spectroscopy of the astronomical anion CN⁻," *J.Chem.Phys.* **153**, 184309 (2020).
- ³²Agúndez, M., Cernicharo, J., Guélin, M., Kahane, C., Roueff, E., Klos, J., Aoiz, F. J., Lique, F., Marcelino, N., Goicoechea, J. R., González García, M., Gottlieb, C. A., McCarthy, M. C., and Thaddeus, P., "Astronomical identification of CN⁻, the smallest observed molecular anion," *A&A* **517**, L2 (2010).
- ³³L. González-Sánchez, B. P. Mant, R. Wester, and F. A. Gianturco, "Rotationally inelastic collisions of CN⁻ with He: Computing cross sections and rates in the interstellar medium," *ApJ* **897**, 75 (2020).
- ³⁴J. Klos and F. Lique, "First rate coefficients for an interstellar anion: application to the CN⁻-H₂ collisional system," *MNRAS* **418**, 271–275 (2011).
- ³⁵L. González-Sánchez, E. Yurtsever, B. P. Mant, R. Wester, and F. A. Gianturco, "Collision-driven state-changing efficiency of different buffer gases in cold traps: He(¹S) Ar(¹S) and p-H₂(¹Σ) on trapped CN⁻(¹Σ)," *Phys.Chem.Chem.Phys.*, Advance Article (2020), 10.1039/D0CP03440A.
- ³⁶S. Petrie, "Novel pathways to CN⁻ within interstellar clouds and circumstellar envelopes: implications for is and cs chemistry," *Mon. Not. R. Astron. Soc.* **281**, 137–144 (1996).
- ³⁷C. Romanzin, E. Louarn, J. Lemaire, J. Zabka, M. Polasek, J.-C. Guillemin, and C. Alcaraz, "An experimental study of the reactivity of CN⁻ and C₃N⁻ anions with cyanoacetylene (HC₃N)," *Icarus* **268**, 242–252 (2016).
- ³⁸S. Jerosimić, F. A. Gianturco, and R. Wester, "Associative detachment (AD) paths for H and CN⁻ in the gas-phase: astrophysical implications," *Phys. Chem. Chem. Phys.* **20**, 5490 (2018).
- ³⁹M. Satta, F. A. Gianturco, F. Carelli, and R. Wester, "A quantum study of the chemical formation of cyano anions in inner cores and diffuse regions of interstellar molecular clouds," *ApJ* **799**, 228–235 (2015).
- ⁴⁰L. Biennier, S. Carles, D. Cordier, J.-C. Guillemin, S. D. Le Picard, and A. Faure, "Low temperature reaction kinetics of CN⁻ + HC₃N and implications for the growth of anions in titan's atmosphere," *Icarus* **227**, 123–131 (2014).
- ⁴¹A. J. Coates, F. J. Crary, G. R. Lewis, D. T. Young, J. H. Waite Jr., and E. C. Sittler Jr., "Discovery of heavy negative ions in Titan's ionosphere," *Geophys. Res. Lett.* **34**, L22103 (2007).
- ⁴²V. Vuitton, P. Lavvasb, R. V. Yelle, M. Galand, A. Wellbrock, G. R. Lewis, A. J. Coates, and J. E. Wahlund, "Negative ion chemistry in Titan's upper atmosphere," *Planet. Space Sci.* **57**, 1558–1572 (2009).
- ⁴³A. McKellar, "Evidence for the molecular origin of some hitherto unidentified interstellar lines," *PASP* **52**, 187 (1940).
- ⁴⁴H. Burton, R. Mysliwiec, R. Forrey, B. Yang, P. Stancil, and N. Balakrishnan, "Fine-structure resolved rotational transitions and database for CN+H₂ collisions," *Mol. Astrophys.* **11**, 23–32 (2018).
- ⁴⁵F. Lique, A. Spielfiedel, N. Feautrier, I. F. Schneider, J. Klos, and M. H. Alexander, "Rotational excitation of CN($X^2\Sigma^+$) by He: Theory and comparison with experiments," *J. Chem. Phys.* **132**, 024303 (2010).
- ⁴⁶F. Lique and J. Klos, "Hyperfine excitation of CN by He," *MNRAS* **413**, L20–L23 (2011).
- ⁴⁷Y. Kalugina, F. Lique, and J. Klos, "Hyperfine collisional rate coefficients of CN with H₂($j = 0$)," *MNRAS* **422**, 812 (2012).
- ⁴⁸Y. Kalugina, J. Klos, and F. Lique, "Collisional excitation of CN($X^2\Sigma^+$) by para- and ortho-H₂: Fine-structure resolved transitions," *J. Chem. Phys.* **139**, 074301 (2013).
- ⁴⁹Y. Kalugina and F. Lique, "Hyperfine excitation of CN by para- and ortho-H₂," *MNRAS* **446**, L21–L25 (2015).
- ⁵⁰J. L. Doménech, O. Asvany, C. R. Markus, S. Schlemmer, and S. Thorwirth, "High-resolution infrared action spectroscopy of the fundamental vibrational band of CN⁺," *J. Mol. Spec.* **374**, 111375 (2020).
- ⁵¹B. Anusuri, "Rotational excitation of cyanogen ion, CN⁺ ($X^1\Sigma^+$) by He collisions," *Comput. Theor. Chem.* **1176**, 112748 (2020).
- ⁵²H.-J. Werner, P. J. Knowles, G. Knizia, F. R. Manby, and M. Schütz, "MOLPRO: a general-purpose quantum chemistry program package," *WIREs Comput. Mol. Sci.* **2**, 242–253 (2012).
- ⁵³H.-J. Werner, P. J. Knowles, G. Knizia, F. R. Manby, M. Schütz, *et al.*, "Molpro, version 2019.2, a package of ab initio programs," (2019), see <https://www.molpro.net>.
- ⁵⁴C. Hampel, K. A. Peterson, and H.-J. Werner, "A comparison of the efficiency and accuracy of the quadratic configuration interaction (QCISD), coupled cluster (CCSD), and brueckner coupled cluster (BCCD) methods," *Chem. Phys. Lett.* **190**, 1–12 (1992).
- ⁵⁵M. J. O. Deega and P. J. Knowles, "Perturbative corrections to account for triple excitations in closed and open shell coupled cluster theories," *Chem. Phys. Lett.* **227**, 321–326 (1994).
- ⁵⁶D. E. Woon and T. H. Dunning Jr, "Gaussian basis sets for use in correlated molecular calculations. iii. the atoms aluminum through argon," *J. Chem. Phys.* **98**, 1358 (1993).
- ⁵⁷D. E. Woon and T. H. Dunning Jr, "Gaussian basis sets for use in correlated molecular calculations. iv. calculation of static electrical response properties," *J. Chem. Phys.* **100**, 2975 (1994).
- ⁵⁸R. J. Le Roy, "LEVEL: A computer program for solving the radial Schrödinger equation for bound and quasibound levels," *J. Quant. Spectrosc. Radiat. Transf.* **186**, 167 (2017).
- ⁵⁹J. S. A. Brooke, R. S. Ram, C. M. Western, G. Li, D. W. Schwenke, and P. F. Bernath, "Einstein coefficients and oscillator strengths for the A ²Π – X²Σ⁺(red) and B²Σ⁺ – x²Σ⁺ (violet) systems and rovibrational transitions in the X²Σ⁺ state of CN," *ApJS* **210**, 23 (2014).
- ⁶⁰H. J. Werner and P. J. Knowles, "A second order multiconfiguration SCF procedure with optimum convergence," *J. Chem. Phys.* **82**, 5053 (1985).
- ⁶¹P. J. Knowles and H. J. Werner, "An efficient second-order MC SCF method for long configuration expansions," *Chem. Phys. Lett.* **115**, 259 (1985).
- ⁶²K. R. Shamasundar, G. Knizia, and H.-J. Werner, "A new internally contracted multi-reference configuration interaction method," *J. Chem. Phys.* **135**, 053101 (2011).

- ⁶³R. A. Kendall, T. H. Dunning Jr, and R. J. Harrison, "Electron affinities of the first-row atoms revisited. systematic basis sets and wave functions," *J. Chem. Phys.* **96**, 6796 (1992).
- ⁶⁴A. K. Wilson and T. H. van Mourik, T amd Dunning, "Gaussian basis sets for use in correlated molecular calculations. vi. sextuple zeta correlation consistent basis sets for boron through neon," *Theochem* **388**, 339–349 (1996).
- ⁶⁵S. F. Boys and F. Bernardi, "Calculation of small molecular interactions by differences of separate total energies - some procedures with reduced errors," *Mol. Phys.* **19**, 553 (1970).
- ⁶⁶H.-J. Werner, B. Follmeg, and M. Alexander, "Adiabatic and diabatic potential energy surfaces for collisions of CN ($X^2\Sigma^+, A^2\Pi/$) with He," *J. Chem. Phys.* **89**, 3139 (1988).
- ⁶⁷C. Gaiser and B. Fellmuth, "Polarizability of helium, neon, and argon: New perspectives for gas metrology," *Phys. Rev. Lett.* **120**, 123203 (2018).
- ⁶⁸G. Saidani, Y. Kalugina, A. Gardez, L. Biennier, R. Georges, and F. Lique, "High temperature rection kinetics of CN($v = 0$) with C₂H₄ and C₂H₆ and vibrational relaxation of CN($v = 1$) with Ar and He," *J. Chem. Phys.* **138**, 124308 (2013).
- ⁶⁹D. López-Durán, E. Bodo, and F. A. Gianturco, "ASPIN: An all spin scattering code for atom-molecule rovibrationally inelastic cross sections," *Comput. Phys. Commun.* **179**, 821 (2008).
- ⁷⁰A. M. Arthurs and A. Dalgarno, "The theory of scattering by a rigid rotator," *Proc. R. Soc. A* **256**, 540 (1960).
- ⁷¹D. E. Manolopoulos, "An improved log derivative method for inelastic scattering," *J. Chem. Phys.* **85**, 6425 (1986).
- ⁷²R. Martinazzo, E. Bodo, and F. A. Gianturco, "A modified variable-phase algorithm for multichannel scattering with long-range potentials," *Comput. Phys. Commun.* **151**, 187 (2003).
- ⁷³B. P. Mant, F. A. Gianturco, L. González-Sánchez, E. Yurtsever, and R. Wester, "Rotationally inelastic processes of C₂⁻ ($^2\Sigma_g^+$) colliding with He (1S) at low-temperatures: *Ab Initio* interaction potential, state-changing rates and kinetic modelling," *J. Phys. B: At. Mol. Opt. Phys.* **53**, 025201 (2020).
- ⁷⁴B. P. Mant, F. A. Gianturco, R. Wester, E. Yurtsever, and L. González-Sánchez, "Thermalization of C₂⁻ with noble gases in cold ion traps," *J. Int. Mass Spectrom.* **457**, 116426 (2020).
- ⁷⁵S. Kato, V. M. Bierbaum, and S. R. Leone, "Laser fluorescence and mass spectroscopic measurements of vibrational relaxation of N₂⁺(v) with He, Ne, Ar, Kr and Xe," *Int. J. Mass Spec. Ion Proc.* **149/150**, 469 (1995).
- ⁷⁶E. E. Ferguson, "Vibrational quenching of small molecular ions in neutral collisions," *J. Phys. Chem.* **90**, 731 (1986).
- ⁷⁷E. I. Dashevskaya, I. Litvin, E. E. Nikitin, and J. Troe, "Semiclassical extension of the Landau-Teller theory of collisional energy transfer," *J. Chem. Phys.* **125**, 154315 (2006).
- ⁷⁸T. P. Snow and M. B.J., "Diffuse atomic and molecular clouds," *Annu.Rev. Astronom. Astrophys.* **44**, 367–414 (2006).
- ⁷⁹M. Agúndez and J. Cernicharo, "Oxygen chemistry in the CSE of the carbon-rich star irc+10216," *ApJ* **650**, 374–393 (2006).

Rotational state-changing collisions of C_2H^- and C_2N^- anions with He under interstellar and cold ion trap conditions: a computational comparison.

Jan Franz,¹ Barry Mant,² Lola González-Sánchez,³ Roland Wester,² and Franco A. Gianturco^{2, a)}

¹⁾*Department of Theoretical Physics and Quantum Informatics, Faculty of Applied Physics and Mathematics, Gdańsk University of Technology, ul. Narutowicza 11/12, 80-233 Gdańsk, Poland*

²⁾*Institute for Ion Physics and Applied Physics, University of Innsbruck, Technikerstr. 25/3, 6020 Innsbruck, Austria*

³⁾*Departamento de Química Física, University of Salamanca, Plaza de los Caídos sn, 37008 Salamanca, Spain*

(Dated: 26 February 2020)

We present an extensive range of quantum calculations for the state-changing rotational dynamics involving two simple molecular anions which are often included within evolutionary analysis of chemical networks in the Interstellar environments, C_2H^- ($X^1\Sigma^+$) and C_2N^- ($X^3\Sigma^-$). The same systems are also of direct interest in modelling selective photo-detachment (PD) experiments in cold ion traps where the He atoms function as the chief buffer gas at the low trap temperatures. This study employs accurate, ab initio calculations of the interaction potential energy surfaces (PESs) for these anions, treated as Rigid Rotors (RR) and the He atom to obtain a wide range of state-changing quantum cross sections and rates at temperatures up to about 100K. The results are analysed within both physical contexts to show differences and similarities between the state-changing dynamics of the two systems.

I. INTRODUCTION

The discovery of carbon chain anions in interstellar and circumstellar media has triggered and stimulated a large number of theoretical and experimental studies on these species (e.g. see reference [1,2]). Their structures and spectral features, as well as the clarification of their importance and of their role in interstellar chemistry, and in gas phase ion-molecule reactions in general, have therefore also attracted many specific studies [3-5] on their behaviour.

The possible, and likely, existence of anions in astrophysical sources was first predicted theoretically and considered in earlier chemical models [6,7], although the first negative hydrocarbon $C_6H_6^-$ was only detected in 2006 [8], thereby also solving the problem of the unidentified lines discovered by Kawaguchi et al. [9]. That identification was soon followed by the detection of other negatively charged species like C_4H^- [10], C_8H^- [11,12], C_3N^- [13], C_5N^- [4], and CN^- [14]. The majority of these species were first detected in a well observed Circumstellar Envelope (CSE) IRC+10216, although these and other hydrocarbon anions were also discovered later on in other molecular clouds [15]. As it is to be expected, the study and search for interstellar anions of both simple and increasingly more complex structural properties is still current and relevant. More specifically, a simple species like C_2H^- ($X^1\Sigma^-$), has been expected to be amenable to observation with the new astrophysical instruments such as ALMA, especially since it had been already observed as a stable molecule in laboratory experiments [16,17]. Furthermore, its parent neutral form C_2H ($X^2\Sigma^+$) has already been a well-known astrophysical molecule discovered by observation as early as 1974 [18], thereby suggesting that the correspond-

ing C_2H^- anion should also be present, although perhaps as only a very low-abundance species, a fact justified in terms of its high chemical reactivity and therefore expected rapid destruction upon formation. Actual current numerical models predict, in fact, that the larger carbon chain anion formations should be in any case more probable than those for similar smaller chains as the C_2H^- [19], hence somehow supporting the difficulties for its observation.

In spite of the fact that the actual origin of many of the hydrocarbon anions has not yet been solved, it is generally accepted that gas-phase processes are crucial for their formation and therefore the many observed hydrocarbon radicals C_nH may also be the main precursors of the formation of C_nH^- anions through electron attachment or association processes, whereas associative detachment processes would contribute to the generation of initial, neutral C_nH species. As an example, a new mechanism for the formation of C_2H^- from C_2H_2 has been proposed not long ago [1] from laboratory experiments.

Along similar lines, another small C-bearing molecule, the neutral CCN radical ($X^2\Pi_r$) has been also detected earlier on in the interstellar medium [20], where the molecule was observed at the 1 – 2 mK level toward the same circumstellar envelope (CSE) of IRC + 10216 already mentioned earlier, using the facilities of the Arizona Radio Observatory (ARO). Lambda doublets of the $J = 4.5 \rightarrow 3.5$ and the $J = 6.5 \rightarrow 5.5$ transitions at 106 GHz and 154 GHz in the $\Omega = 1/2$ ladder were measured with the ARO 12 m telescope, as well as the $J = 9.5 \rightarrow 8.5$ lines near 225 GHz, using the ARO Sub-Millimeter Telescope (SMT) [20]. Considering other species in the same environment, it is interesting to note that the $[CN]/[CCN]/[C_3N]$ abundance ratio was found to be $\sim 500 : 1 : 50$, thus indicating again one could expect a rather low abundance for the neutral radical CCN. For the corresponding anionic counterpart, however, no observational evidence within the same CSE has been reported thus far, also suggesting a low abundance of the latter once formed within

^{a)}Electronic mail: francesco.gianturco@uibk.ac.at

that chemical network.

In spite of this absence of direct detection, both the above anionic molecules, CCN^- and CCH^- , have been the object of several laboratory studies which have analysed in some detail the photo-detachment (PD) mechanisms of these species and several other structural properties [21-26]. Furthermore, in general terms we should note here that possible astrophysical abundances of either observed or not yet observed species have to be understood in terms of molecular stabilities, reaction probabilities and of both radiative and collisional excitations and relaxation of internal molecular modes: the accurate knowledge of all these facts can indeed help us to better explain the existence of a molecule and the probability of it being observed. The molecular stability and the spectroscopic properties of both the C_2H^- and C_2N^- anions been studied in various earlier investigations [22,23,26], while the modelling of molecular emission in the ISM environments where they could be expected to exist requires collisional rate coefficients with the most abundant interstellar species like He and H_2 . Collisional data have been already presented for the C_2H^- anion interacting with He [27], while no corresponding calculations, as far as we know, exist for the collisional rotation-state changes of C_2N^- interacting with He. The actual ab initio PES is also not known for that system. The quantum dynamics of both these anions, besides not being extensively studied under CSE conditions, has also been only partially discussed under the operating low temperatures of ion cold traps [28]. The present work is therefore directed to acquiring novel knowledge about the quantum dynamics of C_2N^- in collision with He under both astrochemical and cold ion trap conditions, further implementing a comparison between its dynamical behaviour and that of the C_2H^- polar anion under similar conditions.

The following Section will only briefly remind readers about the features of the anisotropic potential energy surface involving C_2H^- and He atoms, since it has been presented and analysed already in earlier work [27]. It will instead present in greater details the new calculations of the ab initio points related to the Rigid Rotor (RR) PES associated to the interaction between C_2N^- ($X^3\Sigma^-$) and the neutral He atom. The two interaction potentials will then be compared and their level of spatial anisotropy will be analysed and discussed.

The next Section 3 will present the state-changing rotationally inelastic cross sections for both systems and discuss the effects from spin-spin and spin-rotation structural effects on the C_2N^- system via à vis the C_2H^- ($X^1\Sigma^+$) system. The corresponding inelastic rates at the temperatures of interest will also be presented, compared and discussed. The following Section 4 shall examine the possible evolutionary dynamics of C_2N^- anions under the conditions of a cold trap when they are undergoing laser photo-detachment processes. A comparison with the corresponding behaviour of the C_2H^- system will also be presented and discussed. Our present conclusions will be given in Section 5.

II. FEATURES OF THE AB INITIO INTERACTIONS OF THE PRESENT ANIONS WITH HE ATOMS

As mentioned in the previous Section, the electronic ground state of C_2N^- was taken to be ($X^3\Sigma^-$) as indicated to be in earlier work [22]. The molecular geometry of this linear anion is with $r_{CC} = 1.344 \text{ \AA}$ and 1.207 \AA and was given in the experiments from Garand et al. in ref. [22]. We have optimized the molecular geometry using the MRCI + Davidson correction [29] and employing the aug-cc-pVQZ basis set. The final values of the same bond distances have been the following: $r_{CC} = 1.360 \text{ \AA}$ and $r_{CN} = 1.212 \text{ \AA}$. The ab initio calculations of the 2D grid of points in the space (R, theta) were carried out with the program package MOLPRO 2012 of ref. [29]. For all the present calculations we have employed the internally-contracted multi-reference configuration interaction method (IC-MRCI) [30,31], using the aug-cc-pVQZ basis set [32] on all atoms. The reference space for the MRCI calculations consists of a complete - active space by distributing 14 electrons in 15 orbitals. All single and double excitations from the reference configurations are included in the variational calculation. The effect of quadruple excitations is estimated via the Davidson correction [29]. The angular grid involved calculations of radial `cut` every 5° , from 0° to 180° . The radial grid included a higher density of points around the various minima regions at each selected angle. The total number of radial points was: 44. The global minimum for the complex was found at a distance of around 6.7 Bohr from the centre-of-mass, located at an angle of around 80° , with a well's depth of around 58 cm^{-1} . The data shown by the two panels of Figure 1 provide a pictorial view of the new PES calculated for the C_2N^- /He system (upper panel), while it also shows for comparison the PES already calculated in earlier work for the similar anion of C_2^- interacting with He (from ref. [27]). One clearly sees from the two panels the expected similarities between the two interaction potentials since both exhibit the presence of the minimum structure of their complex with He to be slightly off the C_{2v} geometry and at similar values of distances from the c.-of-m. in each complex. Furthermore, given the larger number of electrons in the C_2N^- case, the corresponding well appears to be deeper than that for the C_2H^- /He complex [27]. Both potentials will be asymptotically driven by the polarizability term involving the spherical, dipole polarizability of the He partner and therefore will behave very similarly in their long-range regions because of it. The localization of the excess charge provided by the extra bound electron of the anion is also an interesting item for the new CCN^- /He PES discussed here. The Mulliken charges in the asymptotic situation (e.g. with the helium at a distance of 50 bohr from the c.-o.-m. of the anionic target) turn out to be as follows (when computed with the MRCI // aug-cc-pVQZ of the post-HF treatment): $C_1 = -0.59049$; $C_2 = +0.22532$; $N_1 = -0.63483$. Here C_2 is the Carbon atom in the middle of the molecule, so that the geometry of CCN^- is given as: $C_1-C_2-N_1$, with no extra charge on the interacting He atom, as expected. The direction and value of the dipole moment are therefore given as: 2.1818 Debye, placed along the positive direction of the molecular z-axis from the C_1 -end of the

FIG. 1. Computed PESs for the two molecular anions of the present study. The data are presented as in-plane maps in 2D with $r \cos \theta$ and $r \sin \theta$ as coordinates. Energy levels in cm^{-1} . Upper panel: C_2N^- from present calculations; lower panel: C_2H^- from ref. [27].

molecule. Another type of presentation of the relevant PES for both systems could be done by numerically generating the radial coefficients of the multipolar expansion of the Rigid Rotor (RR) 2D potential energy surfaces:

$$V(r = r_e, R, \theta) = \sum_{\lambda} V_{\lambda}(R) P_{\lambda}(\cos \theta) \quad (1)$$

where r_e is the geometry of the equilibrium structure of the anion, already discussed earlier, and the sum over the contributing lambda values went up to 19, although only the dominant, stronger terms are shown in Figure 2. The panels of that figure also compare the present findings for C_2N^- with the earlier data for C_2H^- from ref. [27].

The radial coefficients presented in that figure underline once more the similarities between the two systems, for which the overall spatial anisotropy is chiefly controlled by lambda = 1, 2 and 3 terms. This indicates that the $\Delta N = 1$ transitions between rotational levels will be those for which the acting torque from the anisotropic PES will be the strongest, followed by the $\Delta N = 2$ transitions. Such provisional features will be further discussed when analysing the computed inelastic cross sections and rates. Another important element of distinction / similarity would be the relative spacings in energy between rotational states for both systems. The results from the present calculations are reported by the data of Figure 3.

To simplify the comparison we report only the energy spacing between N -level separations, without showing the spin-

FIG. 2. Computed multipolar coefficients calculated from the initial PES data. Upper panel: lower values of the dominant radial coefficients for the C_2N^- anion; lower panel: same data but for the C_2H^- anion. Energy values in cm^{-1} and distances in \AA .

FIG. 3. Schematic location of the rotational energy levels for the molecular anion of the present study. For the case of C_2N^- ($X^3\Sigma^-$) only the pseudo-singlet levels without splitting effects are shown. See main text for further details.

FIG. 4. Steady-state distributions of relative molecular populations of rotational levels for temperatures up to 30K. Left panel: the C_2N^- anion; right panel: the C_2H^- anion. See main text for further discussion.

spin and spin-rotation splitting for C_2N^- . The sizes of those splitting constants are not known or available as yet and we will be discussing further in the next Section how they will be included in the present study. Their energy splittings would in any event not be visible on the chosen energy scale in that Figure. We clearly see, however, that the density of states over the examined range of about 60 cm^{-1} , which should cover the relevant energy ranges of both the CSE environments and the cold ion traps preparation, is dramatically different between the two systems, with the C_2N^- anion showing a double number of states being accessible within that energy range.

The higher ‘crowding’ of rotational states per unit energy for the latter molecule translates into a higher number of them being significantly populated at equilibrium temperatures in either environments. The comparison between steady-state rotational level populations in the two anions is reported by the two panels in Figure 4, where we clearly see that at temperatures in a cold trap around 25K the anion in the left panel significantly populates levels up to $N = 10$, while the C_2H^- anion on the right panel only has states up to $N = 6$ significantly populated. Such differences of behaviour will be further discussed in the next two Sections when the inelastic cross sections and rates will be discussed and the possible dynamics of laser-induced PD processes in traps will be analysed.

III. QUANTUM CALCULATIONS OF STATE-CHANGING ROTATIONALLY INELASTIC CROSS SECTIONS AND RATES

The inelastic cross sections involving collisional transitions in both the title molecules were calculated using our in-house multichannel quantum scattering code ASPIN, which we have already described in many earlier publications of our group [33-35] and therefore will not be repeated here in detail. The interested readers are referred to the above publications for

consultation.

In the OH^+ ($^3\Sigma^-$) state, we have three levels for each total angular momentum ≥ 1 : the rotational levels are in fact split by spin-spin and spin-rotation coupling effects. In the pure Hund’s case (b) the electronic spin momentum S couples with the nuclear rotational angular momentum N ($N = R$ for a Σ state) to form the total angular momentum j , given by $j = N + S$ [36,37]. As a consequence of that coupling terms, the rotational levels of the molecule may be labelled not only by the above quantum numbers defined in the Hund’s case (b) but also by their parity index ϵ . The levels in molecules of odd multiplicity with parity index equal to +1 are labelled **e**, and those with parity index equal to -1 are labelled **f** [36]. However, we shall omit this index in the following discussion since we shall not be using it in our analysis.

The extensive work we have done on collision of He with a $^3\Sigma^-$ molecule [36,37] have already shown that the $\Delta N \neq 0$ transitions involve much larger energy values than those which cause changes in the spin quantum number S that is responsible for the separations between j states. Thus, one can say that rotational quenching transitions have much larger energy gaps than those which simply cause spin-flipping processes within each N -labelled manifold. In a full close-coupling (CC) approach to the quantum dynamics the molecular Hamiltonian includes, in addition to the rotational contribution, a nuclear coupling contribution which induces hyperfine energy splitting. These splittings are however lower than typically 10^{-3} cm^{-1} , i.e. they are much lower than the rotational spacing and collisional energies investigated in this work, as we shall further show later in this paper. In such situation, the common approach (e.g. see: Alexander & Dagdigan [38]) is to neglect the hyperfine splitting and to decouple the spin wave functions from the rotational wave functions, using a recoupling scheme. This simplifies considerably the dynamic problem which is then reduced to solving the usual spin-less CC equations associated to the more usual $^1\Sigma$ case. This approximate but almost exact ‘recoupling approach’ will be considered as our reference approach in the following calculations, where our results will be compared with those carried out for the exact $^1\Sigma$ case of the C_2H^- molecular anion.

Scattering calculations were carried out for collision energies between 1 and 1000 cm^{-1} using steps of 0.1 cm^{-1} for energies up to 100 cm^{-1} , of 0.2 cm^{-1} for $100\text{-}200\text{ cm}^{-1}$, of 1.0 cm^{-1} for $200\text{-}500\text{ cm}^{-1}$ and of 2 cm^{-1} for $500\text{-}1000\text{ cm}^{-1}$. This fine energy grid was used to ensure that important features such as the many resonances appearing in the cross sections were accurately accounted for and their contributions correctly included when the corresponding rates were calculated, as discussed below. The number of partial waves was increased with increasing energy reaching $J = 100$ for the highest energies considered. Inelastic cross sections were computed for all transitions between $j = 0$ to $j = 12$, which was deemed to be sufficient to model buffer gas dynamics in a cold trap up to about 50 K (see below), while the same range of levels is expected to be the one most significantly populated during low-energy collisional exchanges with He atoms within ISM environments dynamical conditions.

Another quantity that we shall compute from the cross sections is the state-to-state inelastic rotational rates over a range of temperatures from thresholds up to about 100K, to cover the range of T values expected to be significant for processes in the ISM environments we are discussing here. Hence, once the state-to-state inelastic integral cross sections are known, the rotationally inelastic rate constants $k_{j \rightarrow j'}(T)$ can be evaluated as the convolution of the cross sections over a Boltzmann distribution of the relative collision energies. In the equation below, all quantities are given in atomic units:

$$k_{j \rightarrow j'}(T) = \left(\frac{8}{\pi \mu k_b^3 T^3} \right)^{(1/2)} \int_0^\infty E \sigma_{j \rightarrow j'}(E) e^{-E/k_B T} dE \quad (2)$$

Both the calculations of inelastic cross sections and of their corresponding rates over the range of temperatures mentioned earlier have been carried out using the new interaction PES for the C₂N⁻/He system and via the earlier PES already computed for the C₂H⁻/He system [27]. The comparison between our findings for these two systems will be further carried out in this Section by presenting our computed data below.

IV. QUANTUM DYNAMICS OF LASER PHOTODETACHMENT PROCESSES IN COLD TRAPS

The additional process that can take place in cold ion traps [27, 39] where the present anions can be confined, and which we now want to describe specifically for the title molecules of this study, involves the following dynamical steps: (i) collisional population re-distribution among the rotational levels of the anion by interaction with He atoms, as the prevalent buffer gas, at the trap temperature; (ii) switching on the photo-detaching laser after the previous rotational population equilibration has been achieved. One could then be varying its operational wavelength to selectively depopulate different rotational states of the anion present in the trap after the step (i); (iii) further test other operating conditions such as: buffer gas density, trap equilibration temperature, laser power and laser wavelength in order to find the best choices for the state-selective photo-detachment (PD) processes tailored to the present system. We therefore have to know beforehand the state-changing collisional rates for the molecular anion in the trap at different operating temperatures and the kinetics of the evolution of the rotational state populations during collisional equilibration. We further require selecting the values of the PD rates (obtained from the PD cross sections as functions of the initial rotational state, as already discussed by us in [28,39]. As a comment about the calculated cross sections and rate for state-to-state inelastic processes suffices it to say that the dominant inelastic processes we found for the present systems are those for which the state-changing values of $\Delta N \pm 1, 2$ and for which the rates at a temperature of, say 20 K, are of the order of xxxxx in units of cm³ s⁻¹. As a comparison, the corresponding Einstein spontaneous emission coefficients for the C₂H⁻ anion vary to be from about 10⁻³ to 10⁻⁵ smaller than the collisional rates for this system [28].

In order to be modelling the rotational population evolution dynamics, the master equations need to be solved using the collisional thermal rates computed above at each chosen trap temperature and for the range of selected He density:

$$\frac{dn_i(t)}{dt} = \sum_{j \neq i} n_j(t) C_{ji}(T) - n_i(t) \sum_{i \neq j} P_{ij}(T) \quad (3)$$

The quantities $P_{ij}(T)$ are the rates for the destruction of level i , while its formation rates are given by the $C_{ji}(T)$ terms. During the collisional step, i.e. before the laser is switched on, the coefficients are given as: $P_{ij}(T) = \eta_{He} k_{j \rightarrow i}(T)$ and $C_{ji}(T) = \eta_{He} k_{j \rightarrow j'}(T)$. These relationships describes the `collision-driven` time evolution process of thermalisation of the relative populations of the rotational levels of the anion which are populated at the selected buffer gas temperature and for a given density η_{He} in the trap. Once thermalisation is reached and the PD laser is turned on, one needs to modify the above master equations by including the PD rates discussed in the previous section and linked to the PD cross sections:

$$\frac{dn_i(t)}{dt} = \sum_{j \neq i} n_j(t) C_{ji}(T) - n_i(t) \left(\sum_{i \neq j} P_{ij}(T) + K_i^{PD} \right), \quad (4)$$

where K_i^{PD} is the additional destruction rate of the selected level i caused by the PD laser. The set of rates K_i^{PD} is critical in the experiments in general and for the present numerical simulations because they drive the destruction of both the population of one specific rotational level i and of all the molecular ions which have been populating that specific state during the previous thermalisation step in the traps. In the experiments of this study these rates depend on the laser photon flux and on the overlap between the laser beam and the ion cloud within the trap. Since these parameters, as well as the absolute values of the state-to-state PD cross sections, are presently unknown for the title molecular anions, we shall introduce a scaling parameter which we have already discussed in our earlier work [28,40] according to which the relation between the required rate and the estimated cross section is given by:

$$K_{j''}^{PD} = \alpha(v) \sigma_{j''}^{PD}(v) \quad (5)$$

The above scaling parameter is helping us to include in the modelling the relative role of different features of the photo-detachment experiment which are effectively the laser-driven features of the PD dynamics. They include quantities like laser-flux, spatial overlap, etc. which compete with the pure collisional rates that repopulate the anion's rotational levels via its interaction with the buffer gas. This specific aspect of the modelling allows us to simulate either a `collision-dominated` situation or a `PD-dominated` situation whenever the laser strength is markedly varied, as we will be further discussing below. The values of the $\sigma_{j''}^{PD}(v)$ can be obtained through an analysis which we have presented before [28,40] and which will be not repeating here. Briefly, the PD cross section is given as:

$$\sigma_{j''}^{PD}(v) \propto \sum_{J'=0}^{J_{\max}} \left| C_{j''010}^{J'} \right|^2 (E - E_{th})^p \Theta(E - E_{th}). \quad (6)$$

Here $\Theta(E - E_{th})$ is a step function so that only transitions with $E_{th} < E$ are considered, and the Clebsch-Gordan coefficient enforces the selection rule $\Delta J'' = \pm 1$ for the specific PD process under consideration. Since the rotational levels' relative populations initially also sum to one, they have limited effect on the relative sizes of the PD cross sections and the PD curve identified by the above equation. Hence, the most important factors are the selected value for the p exponential parameter and the actual wavelength ν of the laser source with respect to the threshold of the specific electron-detachment process.

V. PRESENT CONCLUSIONS

ACKNOWLEDGMENTS

We wish to acknowledge

VI. REFERENCES

- [1] M.A. Cordiner, T.J. Millar, C. Walsh, E. Herbst, D.C. Lis, T.A. Bell, E. Roueff, *Organic Matter in Space*, in: S. Kwok, S. Sandford (Eds.), *Proceedings IAU Symposium No. 251*, 2008.
- [2] M.A. Cordiner, T.J. Millar, *Astrophys. J.* 697 (2009) 68.
- [3] E. Herbst, Y. Osamura, *Astrophys. J.* 679 (2008) 1670.
- [4] C. Walsh, N. Harada, E. Herbst, T.J. Millar, *Astrophys. J.* 700 (2009) 752.
- [5] B. Eichelberger, T.P. Snow, C. Barckholtz, V.M. Bierbaum, *Astrophys. J.* 667 (2007) 1283.
- [6] A. Dalgarno, R.A. Mc Cray, *Astrophys. J.* 181 (1973) 95. [7] E. Herbst, *Nature* 289 (1981) 656. [8] M.C. McCarthy, C.A. Gottlieb, H. Gupta, P. Thaddeus, *Astrophys. J.* 652 (2006) L141. [9] K. Kawaguchi, Y. Kasai, S. Ishikawa, N. Kaifu, *Publ. Astron. Soc. Japan*, 47 (1995) 853. [10] J. Cernicharo, M. Guélin, M. Agúndez, K. Kawaguchi, M.C. McCarthy, P. Thaddeus, *Astron. Astrophys.* 467 (2007) L37.
- [11] A.J. Remijan, J.M. Hollis, F.J. Lovas, M.A. Cordiner, T.J. Millar, A.J. Markwick-Kemper, P.R. Jewell, *Astrophys. J.* 664 (2007) L47.
- [12] S. Brünken, H. Gupta, C.A. Gottlieb, M.C. McCarthy, P. Thaddeus, *Astrophys. J.* 664 (2007) L43.
- [13] P. Thaddeus et al., *Astrophys. J.* 677 (2008) 1132.
- [14] M. Agúndez et al., *Astron. Astrophys.* 517 (2010) L2.
- [15] N. Sakai, T. Shiino, T. Hirota, T. Sakai, S. Yamamoto, *Astrophys. J.* 718 (2010) L49.
- [16] S. Brünken, A. Gottlieb, H. Gupta, M.C. McCarthy, P. Thaddeus, *Astron. Astrophys.* 464 (2007) L33.
- [17] T. Amano, *J.Chem.Phys.* 129 (2008) 244305.
- [18] K.D. Tucker, M.L. Kutner, P. Thaddeus, *Astrophys. J.* 193 (1974) 5425.
- [19] C. Barckholtz, T.P. Snow, V.M. Bierbaum, *Astrophys. J.* 547 (2001) L171.
- [20] J. K. Anderson and L. M. Ziurys, *Astrophys. J. Lett.*, 795: L1 (2014).
- [21] K. Kawaguchi, T. Suzuki, S. Saito, E. Hirota, *Dye Laser Excitation Spectroscopy of the CCN Radical*, *J. Molec. Spectr.* 106, 320 (1984).
- [22] E. Garand, T. I. Yacovitch, D. M. Neumark, *Slow photoelectron velocity-map imaging spectroscopy of C_2N^- , C_4N^- , and C_6N^-* , *J.Chem.Phys.* 130, 064304(2009).
- [23] X. Huang, T.J. Lee, *J.Chem. Phys.* 131,104301(2009).
- [24] K. M. Ervin, W. C. Lineberger, *Photoelectron Spectra of C⁻ and C₂H⁻*, *J. Phys. Chem.*, 95, 1167 (1991).
- [25] J. Zhou, E. Garand, D.M. Neumark, *Vibronic structure in C₂H and C₂D from anion slow-electron velocity-map imaging spectroscopy*, *J. Chem. Phys.* 127, 114313 (2007).
- [26] M. L. Senent and M. Hochlaf, *Reactivity of anions in interstellar media: detectability and applications*, *Ap.J.*, 768:59 (2013).
- [27] F. Dumouchel, A. Spielfiedel, M.L. Senent, N. Feautrier, *Temperature dependence of rotational excitation rate coefficients of C₂H⁻ in collision with He*, *Chem.Phys.Lett.* 533,6 (2012).
- [28] F. A. Gianturco, L. González-Sánchez, B. P. Mant, R. Wester, *Modeling state-selective photodetachment in cold ion traps: Rotational state “crowding” in small anions*, *J. Chem. Phys.* 151, 144304 (2019).
- [29] Werner, H.-J., Knowles, P. J., Knizia, G., Manby, F. R., Schütz, M., & others, *MOLPRO*, version 2012.1, a package of ab initio programs, For the current version, see <http://www.molpro.net> Woon, D. E., & Dunning, T. H. Jr. 1994, *J. Chem. Phys.*, 100, 2975.
- [30] Werner, H.-J., & Knowles, P. J., *J. Chem.Phys.*, 89, 5803 (1988). [31] Shamasundar, K. R., Knizia, G., & Werner, H.-J., *J. Chem. Phys.*, 135, 054101(2011).
- [32] Woon, D. E., & Dunning, T. H. Jr., *J. Chem. Phys.*, 100, 2975(1994).
- [33] Martinazzo R, Bodo E and Gianturco F A *Comput. Phys. Commun.* 151 187 - 198,(2003).
- [34] Hernández Vera M, Gianturco F A, Wester R, da Silva H and Dulieu O., *Schiller S J.Chem. Phys.* 146 124310 (2017).
- [35] L. González-Sánchez, E. Bodo, and F. A. Gianturco, *Quantum scattering of OH(²Π) with He: Propensity features in rotational relaxation at ultralow energies*, *Phys. Rev. A*, 73, 022703 (2006).
- [36] L. Gonzalez-Sanchez, E. Bodo, and F.A. Gianturco, *Quenching of molecular ions by He buffer loading at ultralow energies: rotational cooling of OH+(³Σ⁻) from quantum calculations*, *Eur. Phys. J. D* 44, 65 - 72 (2007)
- [37] L. Gonzalez-Sanchez, R. Wester, F.A. Gianturco, *Modeling Quantum Kinetics in Ion Traps: State-changing Collisions for OH+ (³Σ⁻) ions with He as a Buffer Gas*, *ChemPhysChem*, 19, 1866 (2018).
- [38] M. H. Alexander, P. J. Dagdigian, *J. Chem. Phys.* 79, 302 (1983).
- [39] D. Hauser, S. Lee, F. Carelli, S. Spieler, O. Lakhmanskaya, E. S. Endres, S. S. Kumar, F. Gianturco, and R. Wester, *Nat. Phys.* 11, 467 (2015).
- [40] F. A. Gianturco, O. Y. Lakhmanskaya, M. Hernandez-Vera, E. Yurtsever, and R. Wester, *Collisional relaxation ki-*

netics for ortho and para NH_2^- under photodetachment in cold ion traps, *Faraday Discuss.*, 212, 117 (2018).